Order-disorder phase transition in $CePt_4In$: Evidence from ^{115}In and ^{195}Pt NMR studies

Bogdan Nowak*

W. Trzebiatowski Institute for Low Temperature and Structure Research, Polish Academy of Sciences, Post Office Box 1410, PL-50-950 Wrocław, Poland

(Received 30 August 2010; revised manuscript received 18 January 2011; published 5 April 2011)

We present the results of nuclear magnetic resonance (NMR) studies on $CePt_4In$ crystallizing at ambient temperature in an ordered cubic $MgCu_4Sn$-type structure (space group F-43*m*, no. 216). The ^{115}In and ^{195}Pt NMR powder spectra have provided microscopic evidence for the occurrence of the phase transition suggested by the specific heat anomaly at $T_0 = 205$ K. Single-site (multiple-site) ^{195}Pt ($I = 1/2$) NMR spectra are observed above (below) T_0, while the single-site ^{115}In ($I = 9/2$) NMR signal disappears below T_0. The Solomon echoes of half-integer quadrupolar nuclei with spin $I = 9/2$ have been observed. The Knight shifts $^{115}K_{iso}(T)$ and $^{195}K_{\alpha}(T)$ ($\alpha = //, \perp$, iso, ax) scale linearly with magnetic susceptibility $\chi(T)$. ^{195}Pt NMR exhibits strong anisotropy of the Knight shift and nuclear spin-lattice relaxation rate due to the huge anisotropy of hyperfine fields ($H_{//}/H \perp$) $\approx$ 43. The $(1/T_1)_{iso}$ are fast and temperature independent for both ^{115}In and ^{195}Pt nuclei, indicating that the spin fluctuation of the *4f* electrons has a local nature at the Ce sites.

DOI: 10.1103/PhysRevB.83.134102 PACS number(s): 76.60.−k

I. INTRODUCTION

RT_4X compounds (R indicates rare earths, T indicates transition metals, and X indicates In, Mn), to which $CePt_4In$ belongs, have attracted attention due to interesting and specific physical properties they exhibit, for example, heavy fermion behavior of $CePt_4In$,[1–4] a first-order valence phase transition in $YbCu_4In$,[5–7] and prediction of In or Mn rattling modes in $CePt_4In$ and $CeNi_4Mn$, respectively.[3,8] $CePt_4In$ crystallizes in the cubic $MgCu_4Sn$ structure with the space group F-43*m* (no. 216) and the point-group symmetries at Ce, In, and Pt sites are –43*m*, –43*m*, and 3*m*, respectively, as found in recent neutron diffraction study at $T = 300$ K.[3]

More recently, specific heat data obtained on $CePt_4In$ revealed a pronounced λ-like anomaly at $T_0 = 205$ K, suggesting some sort of phase transition.[9] In order to elucidate whether the peak in $C(T)$ at $T_0 = 205$ K corresponds to a phase transition, we have undertaken a detailed study of ^{115}In and ^{195}Pt NMR measurements. NMR differs from x-ray diffraction in that it is sensitive to local symmetry, as opposed to long-range symmetry. In particular, the NMR of quadrupolar nuclei ^{115}In ($I = 9/2$) might provide new insights into structural disorder of local sites in $CePt_4In$, for example, since NMR is sensitive to local-site environments rather than the bulk environment. An important question in $CePt_4In$ is whether there is a structural distortion at T_0, either external (i.e., a reduction in the total symmetry, e.g., from cubic to tetragonal) or internal (i.e., atomic displacement from regular crystallographic positions).

We show that below T_0 the NMR signal of ^{115}In nuclei disappears, and ^{195}Pt ($I = 1/2$) NMR spectra reveal an overlapping of multiple-site lines. For this reason, our present studies of ^{115}In and ^{195}Pt NMR spectra as well as the Knight shifts and nuclear spin-lattice relaxation rates are limited to temperatures above T_0 where single-site NMR spectra are observed for both ^{115}In and ^{195}Pt nuclei.

II. EXPERIMENTAL DETAILS

Synthesis of polycrystalline $CeInPt_4$ and the methods of sample characterization including magnetic susceptibility measurements have been described in Ref. 4. Energy-dispersive x-ray scattering (EDXS) revealed nearly single-phase character of the sample with concentrations 17.13 ± 0.17 at. % Ce, 68.21 ± 0.26 at. % Pt, and 14.65 ± 0.11 at. % In, only slightly different from the ideal atomic ratio, 1:4:1. The powder x-ray diffraction data yielded the lattice parameter $a_0 = 7.6112(2)$ Å, in agreement with the value $a = 7.6129(6)$ Å obtained in a recent neutron diffraction study.[3]

To make the NMR measurements, a rf field penetration of the sample is necessary. The ingots were therefore powdered and were not subjected to further heat treatment after powdering. ^{115}In and ^{195}Pt NMR measurements were performed between 90 K and 293 K using a Bruker Avance DSX 300 spectrometer operating at a field of 7.05*T* and temperature controller ITC-503 (Oxford Instruments Co Ltd.). Quadrature detection and extended-phase cycling procedures were used. We were particularly careful to explore the region near 205 K to search for signatures of the phase transition indicated by the specific-heat experiment.

^{115}In Solomon echoes[10,11] were produced by a sequence of two pulses, $\alpha_{\pm x} - \tau - \beta_{\pm y}$. Since the nuclear gyromagnetic ratios $(\gamma/2\pi)$ of ^{115}In and ^{195}Pt nuclei do not differ considerably, we have used the ^{195}Pt NMR signal in an aqueous solution of H_2PtCl_6 as a calibration standard to estimate the value of rf magnetic field B_1. In all these experiments, $B_1 \approx 54$ Oe, which corresponds to ^{115}In-$\nu_{RF} \approx 50$ kHz.

Preliminary measurements indicated that ^{195}Pt NMR spectra are asymmetric and extend over more than 250 kHz. Such spectra are difficult to irradiate uniformly. Then, in order to record correctly the total spectrum, the so-called frequency-swept ^{195}Pt NMR spectra were obtained point by point by changing the irradiating frequency in steps incremented by 10 kHz. For frequency scans, the low-power NMR signals were generated by a single pulse sequence with a 90° pulse duration of 80 μs, exciting only a very narrow frequency range. The NMR probe was retuned at each point.

According to the International Union of Pure and Applied Chemistry (IUPAC) unified δ scale, the ^{115}In and ^{195}Pt chemical shift (Knight shift) *K* should be determined with

reference to $\Xi\,^{115}\mathrm{In} = 0.21912629$ and $\Xi\,^{195}\mathrm{Pt} = 0.21496784$, respectively.[12,13] Here Ξ is defined as the ratio of the isotope-specific frequency to that of ^{1}H in tetramethylsilane (TMS) in the same magnetic field. However, the old question of reliable reference compound indicating the "zero shift" value in the ^{195}Pt NMR spectra is still open. Several groups exploring the ^{195}Pt NMR in solids use different standards for chemical shift (Knight shift) determination.[14,15] According to the discussion presented in Ref. 15 and references therein, in this paper we express the ^{195}Pt Knight shifts (in %) as $^{195}K_{\alpha} = {}^{195}K_{\alpha}(\Xi\,^{195}\mathrm{Pt}) + 0.63$, where $\alpha = \mathrm{iso}, //, \perp$. The spin-lattice relaxation rates $1/T_1$ were measured using saturation recovery pulse sequences in which the spin-echo pulse sequence was used in the position of a single monitoring 90° pulse. For uniform saturation of the resonance line, the nuclear magnetization recovers exponentially, independently of the magnitude of the nuclear spin. Then, the spin-lattice relaxation time T_1 can be determined by fitting the data to the three-parameter magnetization recovery function $M(t) = M(\infty)[1 - C \times \exp(-t/T_1)]$, where M(t) and $M(\infty)$ represent, respectively, the signal intensity at time t after saturation and at thermal equilibrium. The quantities T_1, $M(\infty)$, and $C \approx 1$ are treated as adjustable parameters.

III. RESULTS AND DISCUSSION

A. NMR spectra

In the cubic $MgCu_4Sn$ structure with the space group F-43m (no. 216), the Ce atoms are considered to occupy the crystallographic 4a (0,0,0) sites, whereas In and Pt atoms occupy exclusively the 4c ($\frac{1}{4},\frac{1}{4},\frac{1}{4}$) and the 16$e$ (x,x,x) sites, respectively. If the x value of the Pt atoms comes close to a special position ($\frac{5}{8},\frac{5}{8},\frac{5}{8}$) as found in a recent neutron-diffraction study at $T = 300$ K,[3] then in the high temperature (HT) phase each In site is effectively surrounded by 12 Pt nearest neighbors at a distance of $(a\sqrt{11})/8$ and four Ce next-nearest neighbors at $(a\sqrt{12})/8$. In such a case, the electric field gradient (EFG) at the indium atom site is equal to zero due to point group symmetry –43m, and no quadrupolar effects are expected. However, they are clearly present in Figs. 1(a) and 1(b) where the quadrupolar (Solomon) echoes[10,11] were excited. This is the first such observation of Solomon echoes for the $I = 9/2$ system. The occurrence of quadrupolar echoes in the HT phase of $CePt_4In$ is the fingerprint of the deviation from perfect cubic symmetry of the structure, most probably connected with some defects and/or structural (chemical) disorder, and can be used as a simple and fast test of the sample quality. Sensitivity of this method is higher than x-ray or neutron diffraction.

The Solomon echo pulse sequence includes two rf pulses separated by a time delay τ and is applied to powder samples to generate the spectrum because satellite transitions are usually lost in the dead time of the receiver during one pulse experiment. In contrast to the Hahn echoes,[16] for Solomon echoes t must be much shorter than the free-induction decay (FID) of the central transition, on which are superimposed the echoes. Multiple Solomon echoes arise from refocusing off-resonance single quantum (1Q) and multiple quantum (MQ) coherences generated by the first pulse.

The number of Solomon echoes and their positions have been predicted in the literature for the three half-integer quadrupole spins ($I = 5/2$, 7/2, and 9/2) for the case when second-order quadrupole interaction is negligible.[10,11,17–21] The considered spin systems were inhomogeneously broadened by magnetic as well as quadrupole interactions, which resulted in the prediction of so-called allowed and forbidden

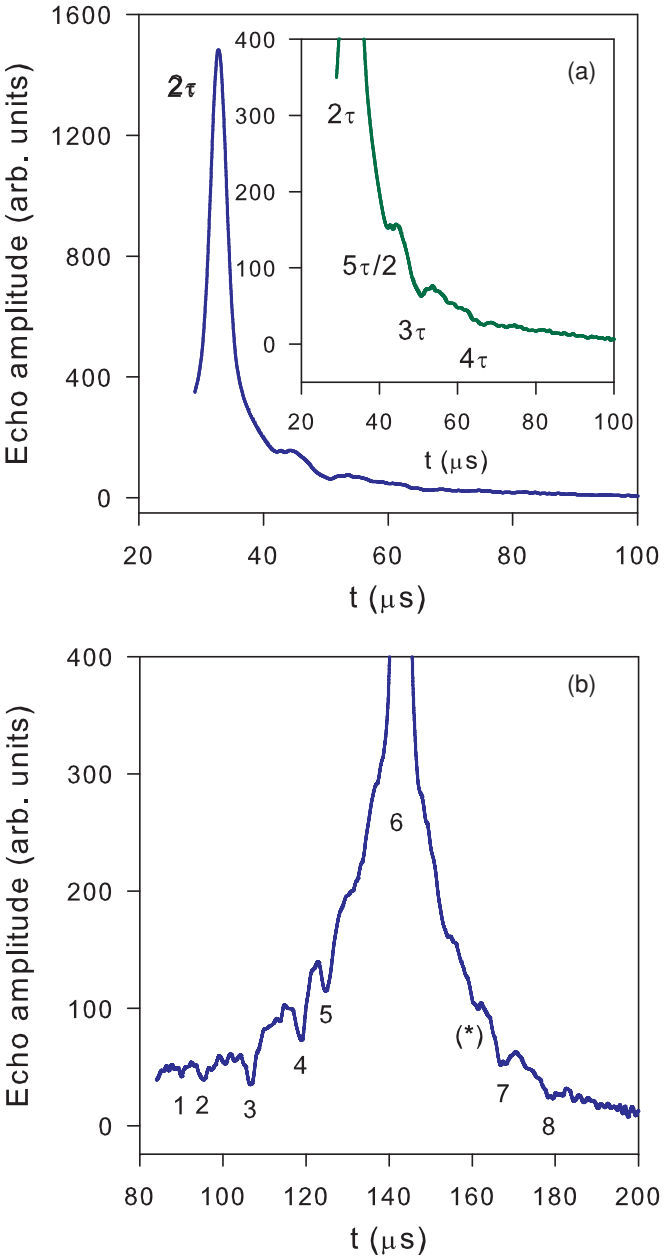

FIG. 1. (Color online) Multiple quadrupolar echoes of ^{115}In ($I = 9/2$) in $CeInPt_4$ recorded at spectrometer frequency of 66.34 MHz ($B_0 = 7.05T$) and $T = 293$ K. The excitation consists of two 2-μs pulses. The second pulse is rf phase-shifted by $\pi/2$. The $\nu_{rf} = 50$ kHz ($B_1 \approx 54$ Oe). The remnants of the free-induction decay after the excitation pulses produce the asymmetry. The two rf pulses are separated by an interpulse delay $\tau = 15$ μs in (a) and $\tau = 70$ μs in (b) to observe all $t < 2\tau$ echoes. Number of scans $NS = 16\,000$ and 64 000 in (a) and (b), respectively. The allowed echoes are observed at times $t = 5\tau/4$ (1), $4\tau/3$ (2), $3\tau/2$ (3), $5\tau/3$ (4), $7\tau/4$ (5), 2τ (6), $7\tau/3$ (7), $5\tau/2$ (8), 3τ (9), and 4τ (10). A kink denoted by (*) in (b) coincides with predicted first forbidden echo at $t = 9\tau/4$.

echoes. More specifically, an allowed echo is the refocusing of two 1Q and two nQ coherences generated by first pulse while a forbidden echo is the refocusing of two couples of nQ coherences. For a comprehensive review, see the paper by P. P. Man[11] and references therein.

For a given spin I, there are $(4I^2-1)(2I-1)/16$ echoes, $(I-1/2)^2$ of which are allowed echoes. All of these echoes are satellite-transition signals, which are superimposed on the FID of the central transition following the second pulse. A spin $I=3/2$ system has no forbidden echo but only one allowed echo located at $t=2\tau$. Here τ represents the separation of the two rf pulses, and time origin starts from the end of the first pulse. For $I>3/2$, several allowed echoes are superimposed at $t=2\tau$. For $I=9/2$, the signal at $t=2\tau$ is composed of four allowed echoes. Also, the signals at $t=3\tau/2$ and 3τ are superpositions of two allowed echoes. Thus, the increasing number of echoes with the spin I makes the experimental study difficult, and experimental examinations are sparse.

Therefore, most of the experimental results verifying the theory of multiple Solomon echoes refer to the spin $I=5/2$ nuclei (mainly ^{27}Al and ^{127}I, both being 100% abundant).[10,17,18,22–24] There are only few papers reporting the experimental results on Solomon echoes in a spin $I=7/2$ system. The first, by Schoep and coworkers,[19] has dealt with ^{51}V in a series of vanadium-based A15 intermetallic compounds V_3X and ^{59}Co in V_3Co. Quite recently, seven allowed echoes were observed at $t=4\tau/3$, $3\tau/2$, $5\tau/3$, 2τ, $5\tau/2$, 3τ, and 4τ for ^{139}La in lanthanum-filled skutterudite $LaOs_4As_{12}$.[25]

To our knowledge, no experimental result has yet been reported on the Solomon echoes in a spin $I=9/2$ system. There are only few nuclei with $I=9/2$. Among them ^{93}Nb, ^{115}In, and ^{209}Bi (all about 100% abundant) are suitable for search of quadrupolar echoes in solids. Appropriate chemical compounds with preferably cubic point-group symmetry at Nb, In, or Bi atom sites are desirable. In our sample, $CePt_4In$, we have met the favorable experimental conditions to excite the quadrupolar Solomon echoes for ^{115}In nuclei with $I=9/2$ and to verify the theoretical prediction on their number and positions.

Imperfections of composition mentioned previously and stress introduced during the sample powdering can be responsible for the presence of weak EFG at the In atom sites. For $I=9/2$, sixteen allowed echoes can be formed. They are expected at eleven values of time,[11] $t=5\tau/4$, $4\tau/3$, $3\tau/2$, $5t/3$, $7\tau/4$, 2τ, $7\tau/3$, $5\tau/2$, 3τ, 4τ, and 5τ, and they were detected in the present experiment, except the 5τ echo due to its very weak amplitude. The amplitude and shape of particular echo signals depend on the phase relationship between the two pulses and their duration. We have realized that the use of two equal-width pulses of 2 μs in duration is optimal for clear visualization of the data in one picture. Such data are presented in Figs. 1(a) and 1(b).

The echoes at $t \gg 2\tau$ can only be observed for short values of τ. However, the resolution is low, and simultaneously the echoes at $t \ll 2\tau$ are lost due to dead time of the receiver [see Fig. 1(a)]. In order to get a better resolution of the different echoes, a long time delay τ between the two 70-μs pulses was used in Fig. 1(b). The echoes reduce strongly due to the short spin-spin relaxation time T_2, which was about 80 μs. With the aid of digital averaging, a satisfying signal-to-noise ratio could be obtained after 64 000 scans, and all predicted echoes for $t<2\tau$ were observed [Fig. 1(b)].

Unlike the composite $3\tau/2$, 2τ, and 3τ echoes, the other signals can be unambiguously associated with one pair of quadrupole transitions.[11] The $5\tau/4$ and $7\tau/4$ echoes are determined solely by $7/2 \leftrightarrow 9/2$ ($-7/2 \leftrightarrow -9/2$) satellite transitions; $4\tau/3$, $5\tau/3$, and $7\tau/3$ echoes are due to the $5/2 \leftrightarrow 7/2$ ($-5/2 \leftrightarrow -7/2$) satellite transitions; the $5\tau/2$ echo is only due to the $3/2 \leftrightarrow 5/2$ ($-3/2 \leftrightarrow -5/2$) satellite transitions; while the 4τ and 5τ echoes depend on inner $1/2 \leftrightarrow 3/2$ ($-1/2 \leftrightarrow -3/2$) satellite transitions. Up to $t=5\tau/3$ as well as for $t=7\tau/3$ and $t=5\tau$, all echoes are solely the allowed echoes. Other allowed echoes can coincide with forbidden ones.

No well-formed solely forbidden echoes were detected, except a weak kink at the position corresponding to the first such echo at $t=9\tau/4$. The origin of the forbidden echoes has not been well understood.[11] The forbidden echoes are not detected for the hard-pulse excitation when the maximum width of the distribution function $f(\nu_q)$ of the quadrupolar frequency $\nu_q = 3eQV_{zz}/2hI(2I-1)$ is small compared to $\nu_{rf}=(\gamma/2\pi)B_1$, that is, $[<\nu_q^2>_{av}]^{1/2}/\nu_{rf} << 1$.[17,19]

Here $C_q = eQV_{zz}/h$ is the quadrupole coupling constant, where Q is the nuclear quadrupole moment, V_{zz} is component of the EFG tensor along the z axis, and $[<\nu_q^2>_{av}]^{1/2}$ represents the rms width of V_{zz}. It is known that disordering has strong effect on the quadrupolar distribution function $f(\nu_q)$ with the result that forbidden echoes can appear.[19]

A very weak forbidden echo at $t=9\tau/4$ can be due to such disordering effects but can also be explained by relatively large value of ν_q resulting in inequality $[<\nu_q^2>_{av}]^{1/2}/\nu_{rf} \geqslant 1$ (soft-pulse excitation). Even for relatively weak EFG at the In site, the ν_q of ^{115}In nuclei is not small, due to considerably large value of the nuclear quadrupole moment $^{115}Q = 81\,(\mathrm{fm})^2$ (Ref. 12).

In principle, the value of ν_q can be estimated from the NMR absorption spectrum. However, it is known that the undistorted NMR absorption spectrum cannot be directly obtained by the Fourier transform of the time-domain signal, which has echoes located at several places in the detection period (multiple echoes).[10,11] The spectrum obtained after appropriate truncation of the time-domain data points is distorted, but fortunately the distribution width of the satellite-transitions is not distorted. Simple Fourier transform without any truncation procedure of the data presented in Fig. 1(b) for $t \geqslant 2\tau$ gives the distorted spectrum shown in Fig. 2 where the satellite spectrum is not resolved. Instead, for the present purposes, a single pulse sequence was applied to excite the FID signal of ^{115}In nuclei. Then, it was Fourier transformed (see inset to Fig. 2). Such a spectrum represents only the central $(1/2) \leftrightarrow (-1/2)$ transition. The spectrum due to satellite transitions is lost in the dead time of the receiver. However, a value of the Knight shift and its temperature dependence shown in Fig. 3 (in which we are mainly interested) can easily and correctly be evaluated.

We have found that the shape and intensity of the ^{115}In NMR signal is temperature independent at high temperatures. The intensity diminishes quickly below $T=220$ K, and the signal disappears below $T=205$ K (Fig. 3). This fact provides

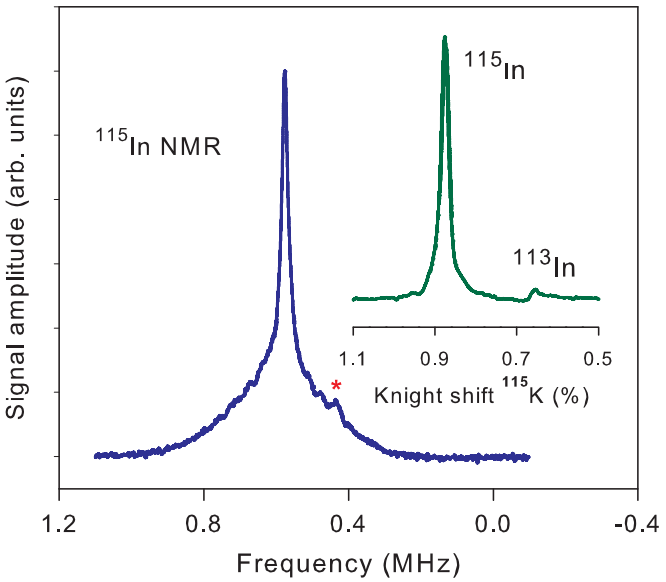

FIG. 2. (Color online) FT-spin echo spectrum of ^{115}In in $CeInPt_4$ obtained without any truncation procedure for the data presented in Fig. 1(b). Zero on the frequency scale corresponds to the zero Knight shift value of ^{115}In nuclei determined with reference to Ξ ^{115}In = 0.21912629 (Refs. 12, 13). Weak signal on the low-frequency site denoted by * is the ^{113}In NMR signal in the sample. Inset: FT-simple pulse spectrum used for the Knight shift determination.

microscopic evidence for the presence of a large EFG at the In atom sites and a large value of C_q due to structural disorder or symmetry lowering below T_0. The possible scenario to explain the disappearance of the ^{115}In NMR signal in $CePt_4In$ seems to be a phase transition from high-T ordered to low-T disordered structure in which the degree of EFG inhomogeneity is so great as to cause essentially complete destruction of the central transition as well as of the satellites. The shape of the specific heat peak on the $C_P(T)$ curve and jump of C_P values measured

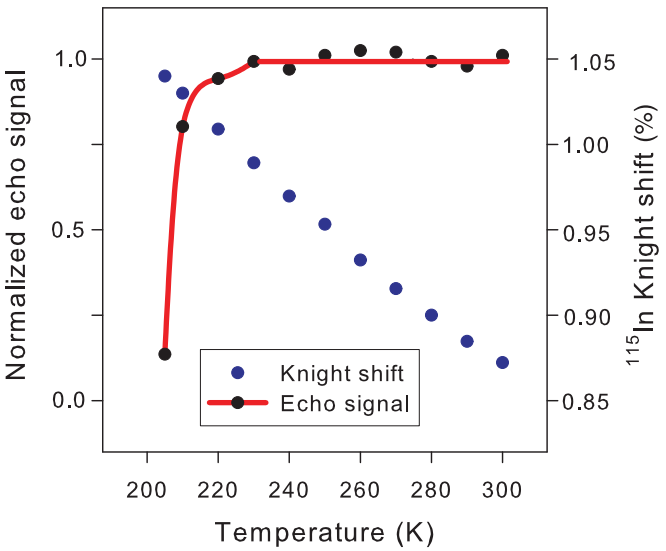

FIG. 3. (Color online) Temperature dependences of the ^{115}In NMR signal and its Knight shift. Below $T_0 = 205$ K, the NMR signal disappears.

below and above T_0 suggest a structural first-order phase transition.[9] A magnetic phase transition can be excluded. Such a conclusion is based on the results of magnetic susceptibility and electrical resistivity of $CePt_4In$,[1–4] which do not reveal any anomaly in their temperature dependencies around T_0. We only note that a dependence of the reciprocal magnetic susceptibility $\chi^{-1}(T)$ is reported in Refs. 1 and 3 to be linear above 100 K, while Pikul *et al.*[2,4] observed such a Curie-Weiss law only above 200 K both for single-crystalline and polycrystalline samples.

The isostructural compound $YbInCu_4$ ($YbCu_4In$ in our notation) shows a first-order valence transition at T_V.[5–7] Above T_V, it is in the stable Yb^{3+} state, while it is in the intermediate valence state with average valence of $Yb^{2.9+}$ below T_V. Experimentally, the two regions are separated by well-defined maximum of the magnetic susceptibility at T_V.[6] The ^{115}In NMR signals are observed both above and below T_V with Knight shift (^{115}K) and nuclear spin-lattice relaxation rates $^{115}(1/T_1)$ exhibiting discontinuous changes at T_V.[6] No such situation is observed in the present case of $CePt_4In$.

A neutron diffraction study at $T = 300$ K indicates that $CePt_4In$ crystallizes in the cubic $MgCu_4Sn$-type structure, which is the ordered version of the $AuBe_5$-type structure.[3] In the disordered version of the $AuBe_5$-type structure, one can assume statistical disorder between Pt and In occupancy on both crystallographic sites.[3] We note that in ordered $YbCu_4In$ where Cu occupies the sites with trigonal $3m$ point-group symmetry, not ^{63}Cu NMR but rather ^{63}Cu NQR was applied mainly due to the considerably large quadrupole coupling constant $^{63}C_q = e^{63}Q^{63}V_{zz}/h \approx 29.5$ MHz.[5,7] For large C_q, the second-order quadrupole interaction leads to a broadening and very pronounced splitting of the central line of the NMR powder spectra and therefore can make the proper determination of the NMR parameters rather difficult. In disordered and powdered alloys, where the quadrupole interaction parameters vary from site to site, this will lead to a very broad and perhaps featureless resonance line. In the extreme case of a very strong quadrupole interaction, it can completely eliminate the NMR signal. If one assumes that V_{zz} values for the Cu site in $YbCu_4In$ and for the Pt site in $CePt_4In$ do not differ considerably, one obtains $^{115}C_q = e^{115}Q^{115}V_{zz}/h > 29.5$ MHz for indium atoms replacing Pt atoms in $CePt_4In$ since $^{115}Q/^{63}Q \approx 3.68$ (Ref. 12). Simultaneously, also the Pt atoms at incorrect positions generate an EFG at In atoms occupying correct positions. For this reason, it is not surprising that our attempts to find the ^{115}In resonance failed in $CePt_4In$ below T_0.

Figure 4 shows the ^{195}Pt NMR spectra obtained for $CePt_4In$ both above and below T_0. The NMR line shape reflects the local symmetry-dependent distribution of ^{195}Pt Knight shifts. We note that at $T > T_0$ a deviation from perfect cubic local symmetry of the structure, responsible for the excitation of Solomon quadrupole echoes of ^{115}In nuclei in the same sample, does not perturb the line shape of single-site ^{195}Pt NMR. The spectra exhibit uniaxially symmetric powder patterns due to anisotropic Knight shift expected for the local trigonal point-group symmetry $3m$ of Pt atoms in the crystal structure of cubic $CePt_4In$ with the space group F-43m (no. 216). This means that number of defects or imperfections of chemical composition is weak. However, below T_0 the ^{195}Pt NMR

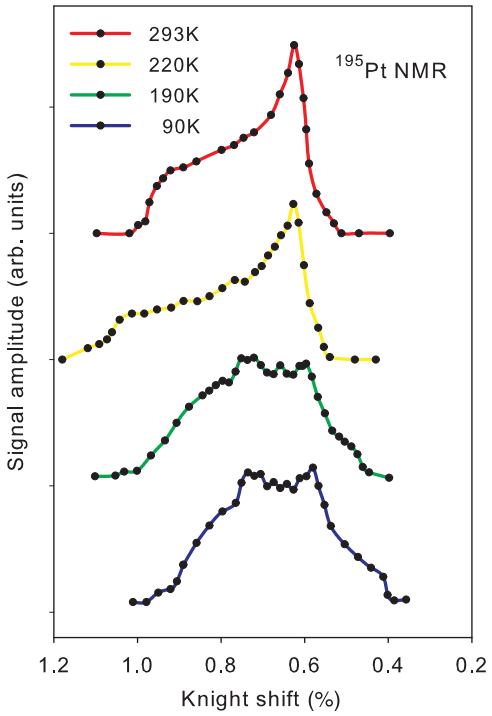

FIG. 4. (Color online) Evolution with temperature of the frequency-swept ^{195}Pt ($I = 1/2$) NMR spectra (see text for the definition of the zero Knight shift value of ^{195}Pt nuclei).

spectra change dramatically (see Fig. 4). Now, an overlapping of multisite NMR lines with nonaxial symmetries is clearly visible. Such pictures can only be understood as a result of structural disorder or local symmetry lowering in the sample, in agreement with our ^{115}In NMR data.

B. Knight shifts

Generally, anisotropic Knight shift depends on anisotropic hyperfine field, an anisotropic magnetic susceptibility, or both. In $CePt_4In$, the temperature dependence of the Knight shift reflects the behavior of the susceptibility of the f electrons, $\chi_f(T)$. Thus, the hyperfine field $H_{\rm hf}$ has two possible origins: a direct dipole field $H^{\rm DIP}$ or a field due to a transferred hyperfine interaction $H^{\rm THI}$. The Knight shift ${}^iK_\alpha$ (i = In, Pt; $\alpha = //, \perp$, iso, ax) of a ^{115}In or ^{195}Pt nucleus due to Ce-ion spins in $CePt_4In$ is proportional to the susceptibility per mol of Ce ions and the hyperfine field at the nuclear site, ${}^iH_\alpha$, where ${}^iH_\alpha$ are the components of the hyperfine field on an i nucleus along the principal axis. In disordered alloys, the Knight shift is inhomogeneous and broadens the NMR line, whereas in ordered intermetallic compounds, the paramagnetic ions contribute only to the average NMR Knight shift ${}^iK_{AV}(T)$. In $CePt_4In$, the static magnetic susceptibility of Ce ions forming a fcc sublattice is isotropic.

Then, the anisotropic NMR line shape reflects the local symmetry-dependent distribution of the Knight shifts through the symmetry-dependent hyperfine couplings at the i site.

The ${}^iH_\alpha$ is temperature independent, and a plot of ${}^iK_\alpha(T)$ versus $\chi_f(T)$ yields a straight line[14] according to

$$ {}^iK_\alpha(T) = {}^iK_{0,\alpha} + {}^iH_\alpha \chi_f(T)/N_{\rm A}\mu_{\rm B} \qquad (1) $$

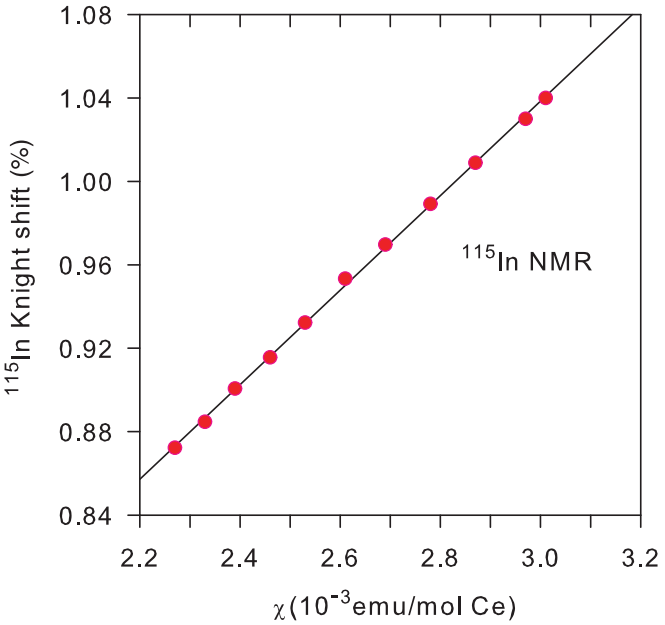

FIG. 5. (Color online) The plot of isotropic Knight shift ^{115}K versus the susceptibility χ with temperature as an implicit parameter for the ^{115}In NMR. The slope of the solid line determines the hyperfine field ${}^{115}H_{\rm iso} = 12.7(1)$ kOe/μ_B.

where ${}^iK_{0,\alpha}$ is constant and N_A and μ_B are the Avogadro's number and Bohr magneton, respectively.

The ^{115}In nuclei occupy positions of nominally tetrahedral –43m point-group symmetry and exhibit only an isotropic Knight shift; the temperature dependence is given in Fig. 3.

In Fig. 5, the ${}^{115}K_{\rm iso}(T)$ was also plotted against $\chi(T)$ with temperature as an implicit parameter for ^{115}In nuclei. Here, we used the $\chi(T)$ data measured at the field 5kOe (Ref. 4) because in the temperature range investigated χ is independent of the field from the measurements up to 50 kOe. Moreover, bulk susceptibility $\chi(T)$ was used instead of $\chi_f(T)$ since temperature independent $\chi_o \ll \chi_f(T)$ and cannot be reliably estimated. The χ_o includes the Larmor and Pauli susceptibilities from the conduction electrons χ_{CE} and orbital χ_{orb} and core diamagnetism $\chi_{\rm dia}$ from the ions. Using Eq. (1), we obtain ${}^{115}K_{0,\rm iso} = 0.359(5)\%$ and ${}^{115}H_{\rm iso} = 12.7(1)$ kOe/μ_B. The positive isotropic component ${}^{115}H_{\rm iso}$ arises from polarized In-5s electrons through the coupling between the In-5s orbital and the Ce-4f spins. Here, the temperature independent ${}^{115}K_{0,\rm iso}$ represents an isotropic part of conduction electron and orbital contributions to ${}^{115}K(T)$. In fact, it is equal to the total experimental ${}^{115}K(LaPt_4In) = 0.35(1)\%$. It is also noted that because of the local tetrahedral symmetry of the In atom site, the dipolar interaction makes no contribution to the observed Knight shift of ^{115}In nuclei and consequently ${}^{115}H_{\rm iso}$ represents a transferred hyperfine field. Below, we also show that the contribution to ${}^{115}(1/T_1)$ in $CePt_4In$ from dipolar interaction is estimated to be at most 1.5% of that from transferred hyperfine interaction.

Above T_0, the ^{195}Pt NMR spectra exhibit uniaxially symmetric powder patterns due to the anisotropic Knight shift expected for the local trigonal point-group symmetry 3m of Pt atoms in the crystal structure of cubic $CePt_4In$ with the space group F43m (no. 216). In Fig. 4, the ^{195}Pt Knight

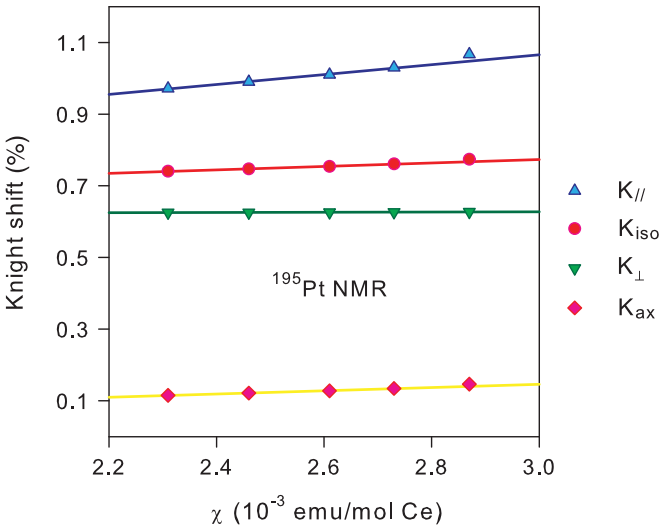

FIG. 6. (Color online) $^{195}K_{\alpha}(T)$ ($\alpha = //, \perp$, iso, ax) versus $\chi(T)$ plots with temperature as an implicit parameter.

shift components perpendicular ($K_{\perp}$) and parallel ($K_{//}$) to the principal axis were derived from the peak maximum and the maximum slope of the shoulder, respectively.

The isotropic and anisotropic (axial) components of the Knight shift were evaluated as

$$K_{\rm iso} = (1/3)(K_{//}+2K_{\perp}) \tag{2a}$$

$$K_{\rm ax}=(1/3)(K_{//}-K_{\perp}) \tag{2b}$$

At $T = 293$ K, $K_{\rm iso} = 0.740(5)\%$ and $K_{\rm ax} = 0.115(5)\%$. With lowering the temperature down to T_0, the single-site axially symmetric line shape is retained. $K_{\perp}$ is nearly constant while $K_{//}$ and thus $K_{\rm iso}$ and $K_{\rm ax}$ slightly increase. The fact that magnetic susceptibility is isotropic implies that anisotropy of hyperfine fields is responsible for the Knight shift anisotropy.

From the relation between the Knight shift and the magnetic susceptibility, we can estimate the hyperfine coupling constants for ^{195}Pt nuclei originating from the 4*f* spins of Ce. In Fig. 6, we plot $^{195}K_{\alpha}$ versus $\chi(T)$ with temperature as an implicit parameter. The linear dependences are clearly seen and can be described by Eq. (1). Evaluated numerical data are presented in Table I.

The isotropic component $^{195}H_{\rm iso}$ represents the transferred hyperfine interaction between the Ce 4*f* orbitals and the Pt 6*s* and 5*d* orbitals. Net spin moment of the 5*d* electrons at the Pt site is parallel to the moment of the 4*f* electrons at the Ce site. These spin-polarized *d* electrons then polarize the inner-core *s* electrons, producing negative hyperfine field through the Fermi contact interaction between the ^{195}Pt nucleus and the core *s* electrons. However, to explain the observed magnitude and positive sign of the transferred hyperfine coupling, involvement of the Pt-6*s* state is necessary. A possible mechanism might be 6*s*(Pt)-4*f*(Ce) mixing, which produces a positive contribution to the hyperfine field at the ^{195}Pt nuclei.

TABLE I. Values of X_{α} ($^{195}K_{0,\alpha}$ and $^{195}H_{\alpha}$) obtained by fitting the experimental $^{195}K_{\alpha}(T)$ to Eq. (1).

	$X_{//}$	$X_{\perp}$	$X_{\rm iso}$	$X_{\rm ax}$
K_0 (%)	0.651(16)	0.618(2)	0.629(6)	0.011(4)
H (kOe/μ_B)	7.73(35)	0.18(5)	2.69(14)	2.52(10)

The anisotropic (axial) component $^{195}H_{\rm ax}$ is of near the same magnitude as $^{195}H_{\rm iso}$. It is ascribed partly to the dipolar coupling between Ce local moments and given Pt nucleus. Extrapolated to $\chi_f(T) = 0$, the values of $^{195}K_{0,\alpha}$ are expected to represent the isotropic positive hyperfine field plus weak anisotropic orbital and dipolar interactions at the Pt nucleus in the absence of 4*f* electrons and should be compared to that of isostructural $LaPt_4In$ without 4*f* electrons. However, the inhomogeneous ^{195}Pt NMR spectrum of $LaPt_4In$ is broad and practically symmetric with $^{195}K_{\rm iso} \approx 0.49\%$, which is distinctly different from $^{195}K_{0,\rm iso} \approx 0.63\%$ in $CePt_4In$.

C. Spin-spin relaxation rates

Intensity of the echoes observed at $t = 2\tau$ was used to determine the transverse spin-spin (phase-memory) times (T_2) of ^{115}In nuclei according to $I = I_o \exp(-2\tau/T_2)$ (Fig. 7). Here, t represents the separation of the two rf pulses exciting an echo. The measured spin-echo phase-memory times $T_2 \sim 80/105$ μs are much longer than echo width $\Delta_{1/2} \sim 10$ μs, so that phase-memory narrowing is negligible and $\Delta_{1/2}$ can only be due to quadrupolar interaction and Knight shift distribution provoked by some structural disorder.

D. Spin-lattice relaxation rates

1. ^{115}*In nuclei*

In the presence of a strong quadrupolar coupling ($C_q = eQV_{zz}/h$), it is difficult to saturate the entire powder-pattern line profile. As mentioned, even for not very large V_{zz}, the C_q can be large for ^{115}In nuclei due to considerably large value of

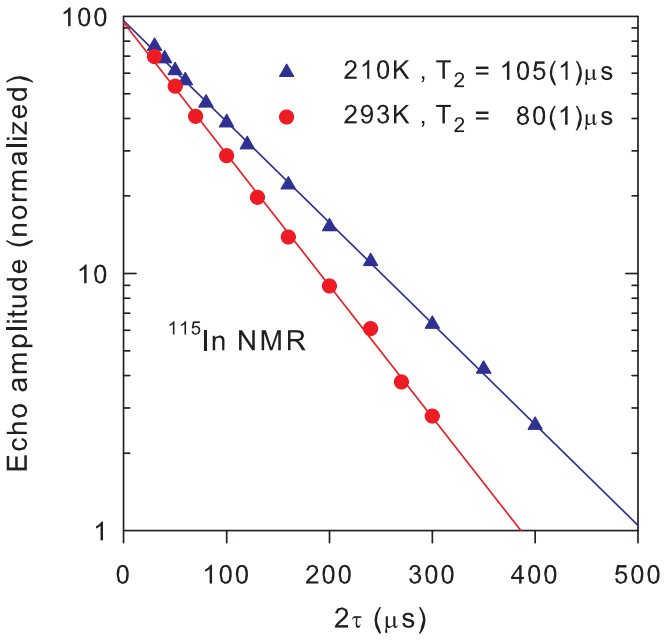

FIG. 7. (Color online) ^{115}In transverse relaxation time T_2.

the nuclear quadrupole moment $^{115}Q = 81$ (fm)^2 (Ref. 12). As a result, spin-echo measurements of central portion of the line do not recover exponentially, but for the present case of ^{115}In nuclei ($I = 9/2$) have a magnetization recovery described as

$$M(t) = M(\infty)[1 - c_1 \exp(-t/T_1) - c_2 \exp(-6t/T_1) - c_3 \exp(-15t/T_1) - c_4 \exp(-28t/T_1) - c_5 \exp(-45t/T_1)], \quad (3)$$

where the appropriate values of the c's are determined by the initial saturation conditions.[26–28] In order to minimize the nonexponential character of the magnetization recovery, we have used a train of short saturation pulses. This procedure uniformly saturates near all the transitions. We did not succeed in achieving complete saturation, but an important part of the magnetization recovers with the time constant T_1.

Typical ^{115}In recoveries in $CePt_4In$ are shown in Fig. 8 for $T = 293$, 250, and 220 K. By about two decades, the plots are linear within an experimental accuracy, indicating that they are well described by a single exponential function. However, the saturation is only 90–96% complete because of the necessity of spreading the rf power over a broad line width. Almost parallel plots indicate that nuclear spin-lattice relaxation rate is temperature independent in the temperature range investigated with $^{115}1/T_1 = 735(45)\ s^{-1}$.

The temperature-independent $1/T_1$ is generally observed for the local moment systems, and such a picture was considered in interpretation of high-temperature magnetic susceptibility of $CePt_4In$.[4]

The contributions to the relaxation rate can be divided into those arising from the local 4f moments and from the conduction electrons at the Fermi energy:

$$1/T_1 = (1/T_1)_{4f} + (1/T_1)_{CE} \quad (4)$$

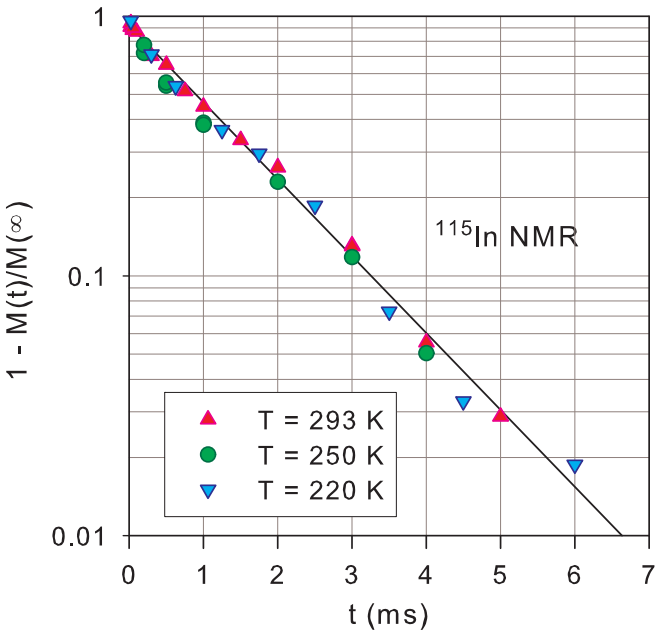

FIG. 8. (Color online) Recovery of the ^{115}In nuclear magnetization as a function of pulse spacing t after the saturation for three temperatures: 293, 250, and 220 K. The solid line represents the fit with temperature-independent $^{115}(1/T_1)_{iso} = 734 \pm 45\ s^{-1}$.

The conduction electron contributions to the relaxation rates of light rare earth-based compounds are usually assumed to be equal to that for La-based ones (without f electrons). A structural disorder at both In and Pt sites in our samples of $LaPt_4In$ precluded reliable determination of relaxation rates. However, since $(1/T_1)_{CE} \propto T$ while observed $1/T_1 \approx$ const in $CePt_4In$, we assume that $(1/T_1)_{CE} \ll (1/T_1)_{4f}$. Generally, $1/T_1$ can be expressed in terms of the wave-vector q-dependent dynamic susceptibility $\chi(q,\omega) = \mathrm{Re}\ \chi(q,\omega) + \mathrm{Im}\ \chi(q,\omega)$ of the fluctuating electronic magnetism[29–32]

$$1/T_1 = \gamma_n^2 k_B T \left(N_A \mu_B^2\right)^{-1} \sum_q |H_{hf}(q)|^2 \mathrm{Im}\chi(q,\omega_n)/\omega_n, \quad (5)$$

where k_B is the Boltzmann constant, γ_n and ω_n are the nuclear gyromagnetic ratio and Larmor frequency, respectively, and ω_n is usually very small compared to characteristic fluctuations rates. $H_{hf}(q)$ is the spatial Fourier transform of the components of the hyperfine coupling tensor between the i nucleus (In or Pt) and the surrounding Ce 4f moments, which generally includes the dipolar as well as the transferred hyperfine interactions. If the electronic fluctuations are not spatially correlated, Im $\chi(q,\omega)$ is independent of q and Im $\chi(q,\omega_n)/\omega_n = \chi_{loc}\ \tau_f$, where χ_{loc} is the local susceptibility, which can be approximated by χ, and $1/\tau_f$ is an effective relaxation rate of Ce 4f moments.

Equation (5) can also be expressed for i nucleus as[31]

$$1/T_1 = \gamma_n^2 k_B T \left(N_A \mu_B^2\right)^{-1} \left[2 \sum_k H_{hf}(k)^2 + \sum_k 4\mu_B^2 r_{jk}^{-6}\right] \chi_{loc} \tau_f, \quad (6)$$

where $H_{hf}(k)$ is the field resulting from transferred hyperfine interaction between the I nucleus at the origin (j) and the Ce 4f moment at k, and r_{jk} is their distance. The second term in the square brackets in Eq. (6) is the dipolar contribution. Although $H_{hf}(k)$ is not known,[30] we assume as usual[31,32] that only the first nearest neighbor Ce 4f moments contribute to the transferred hyperfine field and approximate the factor $\Sigma_k H_{hf}(k)^2$ in Eq. (6) by $z_0({}^i H_{iso}/z_0)^2$. Here, z_0 is the number of the first nearest neighbor Ce ions, and ${}^i H_{iso}$ is taken from the Knight shift measurements. In the structure of $CePt_4In$, the indium atoms occupy tetrahedral interstices in the fcc sublattice of cerium atoms with $z_0 = 4$. Thus, $^{115}H_{iso} = 12.7(1)$ kOe, $\Sigma_k r_{jk}^{-6} = 660.5 a_0^{-6}$ (Ref. 33) and $\Sigma_k 4\mu_B^2 r_{jk}^{-6} = 1.169$ (kOe)^2, indicating that according to Eq. (6) $^{115}(1/T_1)_{DIP}/{}^{115}(1/T_1)_{THI} \approx 0.0145$.

2. ^{195}*Pt nuclei*

Generally, for an anisotropic hyperfine field, both Knight shift and nuclear spin-lattice relaxation rate are anisotropic. In the case of axial symmetry, $1/T_{1,//}$ and $1/T_{1,\perp}$ are expressed as[34]

$$1/T_{1,//} = C(H_\perp)^2 \mathrm{Im}\chi_\perp(\omega_n)/\omega_n, \quad (7a)$$

$$1/T_{1,\perp} = (1/2)C\{(H_\perp)^2 \mathrm{Im}\chi_\perp(\omega_n)/\omega_n + (H_{//})^2 \mathrm{Im}\chi_{//}(\omega_n)/\omega_n\} \quad (7b)$$

with $C = \gamma_n^2 k_B T/N_A \mu_B^2$. In the present case, both static and dynamic magnetic susceptibilities are isotropic, that is, Im $\chi_\perp(\omega_n)/\omega_n = \mathrm{Im}\chi_{//}(\omega_n)/\omega_n$ and anisotropy of $1/T_1$

is determined by anisotropy of the hyperfine coupling constants

$$1/T_{1,\perp}/1/T_{1,//} = [(H_\perp)^2 + (H_{//})^2]/2(H_\perp)^2. \quad (8)$$

Moreover, isotropic and axial components of the relaxation rate fulfill the relations[35]

$$1/T_{1,\mathrm{iso}} = (1/3)(1/T_{1,//} + 2/T_{1,}\perp) \quad (9a)$$

and

$$1/T_{1,\mathrm{ax}} = (1/3)(1/T_{1,//} - 1/T_{1,}\perp) \quad (9b)$$

Since $(H_{//}/H_\perp) \approx 43$ for ^{195}Pt nuclei in $CePt_4In$, the estimated value of $1/T_{1,\perp}$ is about three orders of magnitude larger than that of $1/T_{1,//}$. So, in order to study the nuclear spin-lattice relaxation process of ^{195}Pt nuclei, the NMR signal was sampled only at the peak maximum corresponding to $K_\perp$ for different delay times t after the perturbation of nuclear spins by rf pulses. The^{195}Pt nuclear spin-lattice relaxation rate is practically temperature independent with $^{195}(1/T_1)_\perp = (900 \pm 20)\ s^{-1}$, and these data are presented in Fig. 9. Note that $1/T_{1,iso} \approx (2/3)\ 1/T_{1,\perp}$ for ^{195}Pt nuclei in $CePt_4In$.

For platinum atoms $z_0 = 3$, $^{195}H_{\mathrm{iso}} = 2.7(1)$ kOe. Numerical calculations performed up to $r_{jk} = 50$ Å give $\Sigma_k 4\mu_B^2 r_{jk}^{-6} = 1.204$ (kOe)^2, thus indicating that dipolar contribution to the relaxation rate of platinum nuclei in $CePt_4In$ is not negligible since $^{195}(1/T_1)_{\mathrm{DIP}}/^{195}(1/T_1)_{\mathrm{THI}} = 0.2478$.

Finally, we discuss the disagreement between the experimental and estimated ratio R defined as $^{115}(1/T_1)/^{195}(1/T_1)$. By applying Eq. (6) where Im $\chi(q,\omega)$ is assumed to be independent of q, one obtains

$$R = {}^{115}\gamma_n^2\left[2\sum_k {}^{115}H_{\mathrm{hf}}(k)^2 + \sum_k 4\mu_B^2 r_{jk}^{-6}\right]/{}^{195}\gamma_n^2 \times \left[2\sum_k {}^{195}H_{\mathrm{hf}}(k)^2 + \sum_k 4\mu_B^2 r_{jk}^{-6}\right]. \quad (10)$$

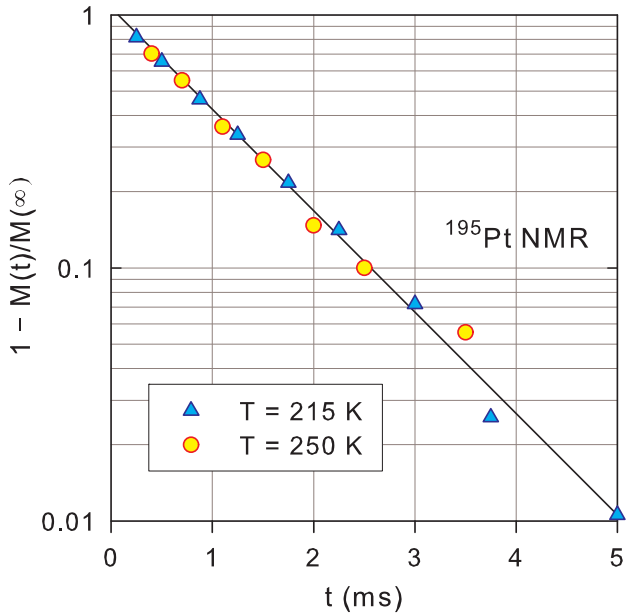

FIG. 9. (Color online) Recovery of the ^{195} Pt nuclear magnetization as a function of pulse spacing t after the saturation at 250 and 215 K. The solid line represents the fit with $^{195}(1/T_1)_\perp = (900 \pm 20)s^{-1}$.

The estimated $R \approx 13.8$ based on the assumption of only the first nearest neighbor contributions to the transferred hyperfine field described earlier is an order of magnitude larger than experimentally observed $R \approx 1.2$. This indicates in turn that the In and Pt THI with Ce $4f$ magnetic dipole moments can be long-ranged, that is, $z_{\mathrm{eff}} > z_0$. We note that MacLaughlin *et al.*[29] obtained $z_{\mathrm{eff}} = 9$ from ^{27}Al NMR in $CeAl_2$, the value to be compared with the crystallographic number of six Ce nearest neighbors to an Al site. However, the use of indium $z_{\mathrm{eff}} = 12$ and platinum $z_{\mathrm{eff}} = 7$ representing the sum of first and second nearest Ce neighbors yields only a slightly lower $R \approx 8.7$. This weak decrease in R is due to the dominance of THI for ^{115}In nuclei.

In conclusion, we state that the ^{115}In and ^{195}Pt NMR powder spectra have confirmed the occurrence of the phase transition suggested by specific heat anomaly at $T_0 = 205$ K. Single-site (multiple-site) ^{195}Pt NMR spectra are observed above (below) T_0, respectively. In contrast to the case of ^{195}Pt NMR ($I = 1/2$), the single-site ^{115}In ($I = 9/2$) NMR signal disappears below T_0. This fact provides microscopic evidence for the presence of EFG at the In atom sites due to structural disorder or symmetry lowering below T_0. Therefore, to better understand the nature of the transition, the series of new bulk measurements should be performed with the main focus on the temperature interval about T_0.

Above T_0, an application of two rf pulse sequences for ^{115}In nuclei ($I = 9/2$) generates multiple quadrupolar (Solomon) echoes. This is first such an observation of Solomon echoes for the $I = 9/2$ system, and details are presented here. Ten of eleven predicted allowed echoes were observed. The occurrence of quadrupolar echoes indicates the deviation from perfect cubic symmetry of the structure even above $T_0 = 205$ K, most probably connected with some defects and/or structural (chemical) disorder. At temperatures above T_0, where the reciprocal magnetic susceptibility $1/\chi$ exhibits linear T dependence (Curie-Weiss law), we have found that the Knight shifts $^{115}K_{\mathrm{iso}}(T)$ and $^{195}K_\alpha(T)$ (α = //, $\perp$, iso, ax) scale linearly with magnetic susceptibility $\chi(T)$ dominated by susceptibility $\chi_f(T)$ of Ce $4f$ magnetic moments.

The nuclear spin-lattice relaxation rates are practically temperature independent for both ^{115}In and ^{195}Pt nuclei. All these results are understood in terms of a conventional local moment picture. The mechanism of Knight shifts and nuclear spin-lattice relaxation is dominated by transferred hyperfine interaction of the ^{115}In and ^{195}Pt nuclei with the $4f$ electrons of the Ce atoms. About 20% contribution to the isotropic relaxation rate from dipolar interaction of nuclei with Ce $4f$ moments is found in the ^{195}Pt NMR.

ACKNOWLEDGMENTS

I express my sincere thanks to A. Pikul for providing the sample of $CePt_4In$ and its characterization by the powder x-ray diffraction and energy dispersive x-ray scattering. It is a pleasure to acknowledge several stimulating and informative discussions with D. Kaczorowski.

*B.Nowak@int.pan.wroc.pl

[1]S. K. Malik, D. T. Adroja, M. Slaski, B. D. Dunlap, and A. Umezawa, Phys. Rev. B **40**, 9378 (1989).
[2]A. P. Pikul, D. Kaczorowski, Z. Bukowski, K. Gofryk, U. Burkhardt, Yu. Grin, and F. Steglich, Phys. Rev. B **73**, 092406 (2006).
[3]A. D. Hillier, D. T. Adroja, S. R. Giblin, W. Kockelmann, B. D. Rainford, and S. K. Malik, Phys. Rev. B **76**, 174439 (2007).
[4]A. Pikul and D. Kaczorowski, Mat. Sci. Poland **26**, 821 (2008).
[5]H. Nakamura, K. Nakajima, Y. Kitaoka, K. Asayama, K. Yoshimura, and T. Nitta, J. Phys. Soc. Jpn. **59**, 28 (1990).
[6]K. Yoshimura, T. Nitta, T. Shimizu, M. Mekata, H. Yasuoka, and K. Kosuge, J. Magn. Magn. Mater. **90/91**, 466 (1990).
[7]T. Koyama, M. Nakamura, T. Mito, S. Wada, and J.L. Sarrao, J. Phys. Condens. Matter **17**, S901 (2005).
[8]I. I. Mazin, Phys. Rev. B **73**, 012415 (2006).
[9]A. Pikul *et al*., (private communication).
[10]I. Solomon, Phys. Rev. **110**, 61 (1958).
[11]P. P. Man, J. Chem. Phys. **106**, 3908 (1997).
[12]R. K. Harris *et al*., Solid State Nucl. Magn. Reson. **22**, 458 (2002), reprinted from Pure Appl. Chem. **73**, 1795 (2001).
[13]R. K. Harris *et al*., Solid State Nucl. Magn. Reson. **33**, 41 (2008), reprinted from Pure Appl. Chem. **80**, 59 (2008).
[14]G. C. Carter, L. H. Bennett, and D. J. Kahan, Prog. Mater. Sci. **20** 295 (1977).
[15]B. Nowak, Solid State Nucl. Magn. Reson. **37**, 36 (2010).
[16]E. L. Hahn, Phys.Rev. **80**, 580 (1950).
[17]J. Butterworth, Proc. Phys. Soc. London **86**, 297 (1965).
[18]I. D. Weisman and L. H. Bennett, Phys. Rev. **181**, 1341 (1969).
[19]G. K. Schoep, H. J. vd. Valk, G. A. M. Frijters, H. B. Kok, and N. J. Poulis, Physica **77**, 449 (1974).
[20]P. P. Man, Z. Naturforsch. A **49**, 89 (1994).
[21]S. Z. Ageev, P. P. Man, and B. C. Sanctuary, Mol. Phys. **88**, 1277 (1996).
[22]C. W. B. Lee and B. C. Sanctuary, J. Magn. Reson. **59**, 189 (1984).
[23]M. S. Krishnan, N. Lee, B. C. Sanctuary, and T. K. Halstead, J. Magn. Reson. **80**, 214 (1988).
[24]N. Lee, B. C. Sanctuary, and T. K. Halstead, J. Magn. Reson. **98**, 534 (1992).
[25]B. Nowak, O. Żogał, Z. Henkie, and M. B. Maple, Solid State Nucl. Magn. Reson. **36**, 209 (2009).
[26]W. W. Simmons, W. J. O'Sullivan, and W. A. Robinson, Phys. Rev. **127**, 1168 (1962).
[27]A. Narath, Phys. Rev. **162**, 320 (1967).
[28]C. Berthier, D. Jerome, and P. Molinie, J. Phys. C: Solid State Phys. **11**, 797 (1978).
[29]D. E. MacLaughlin, O. Peña, and M. Lysak, Phys. Rev. B **23**, 1039 (1981).
[30]D. E. MacLaughlin, J. Magn. Magn. Mater. **47/48**, 121 (1985).
[31]S. Takagi, A. Oyamada, and T. Kasuya, J. Phys. Soc. Jpn. **57**, 1456 (1988).
[32]H. Tanida, S. Takagi, H. S. Suzuki, I. Satoh, and T. Komatsubara, J. Phys. Soc. Jpn. **75**, 074721 (2006).
[33]H. S. Gutowsky and B. R. Mc Garvey, J. Chem. Phys. **20**, 1472 (1952).
[34]F. Borsa, P. Carretta, M. Corti, and A. Rigamonti, Appl. Magn. Reson. **3**, 509 (1992).
[35]J. Aarts, F. R. de Boer, and D. E. MacLaughlin, Physica B **121**, 162 (1983).